




Distinguishing methicillin-resistant *Staphylococcus aureus* from methicillin-sensitive strains by combining Fe₃O₄ magnetic nanoparticle-based affinity mass spectrometry with a machine learning strategy

Wei-Hsiang Ma¹ · Che-Chia Chang^{2,3} · Te-Sheng Lin^{2,4} · Yu-Chie Chen^{1,5} 

Received: 6 February 2024 / Accepted: 30 March 2024
© The Author(s) 2024

Abstract

Pathogenic bacteria, including drug-resistant variants such as methicillin-resistant *Staphylococcus aureus* (MRSA), can cause severe infections in the human body. Early detection of MRSA is essential for clinical diagnosis and proper treatment, considering the distinct therapeutic strategies for methicillin-sensitive *S. aureus* (MSSA) and MRSA infections. However, the similarities between MRSA and MSSA properties present a challenge in promptly and accurately distinguishing between them. This work introduces an approach to differentiate MRSA from MSSA utilizing matrix-assisted laser desorption ionization mass spectrometry (MALDI-MS) in conjunction with a neural network-based classification model. Four distinct strains of *S. aureus* were utilized, comprising three MSSA strains and one MRSA strain. The classification accuracy of our model ranges from ~92 to ~97% for each strain. We used deep SHapley Additive exPlanations to reveal the unique feature peaks for each bacterial strain. Furthermore, Fe₃O₄ MNPs were used as affinity probes for sample enrichment to eliminate the overnight culture and reduce the time in sample preparation. The limit of detection of the MNP-based affinity approach toward *S. aureus* combined with our machine learning strategy was as low as $\sim 8 \times 10^3$ CFU mL⁻¹. The feasibility of using the current approach for the identification of *S. aureus* in juice samples was also demonstrated.

Keywords Fe₃O₄ MNPs · *Staphylococcus aureus* · MRSA · MALDI-MS · Machine learning · Neural network

Wei-Hsiang Ma and Che-Chia Chang contributed equally to this work.

✉ Te-Sheng Lin
teshenglin@nycu.edu.tw

✉ Yu-Chie Chen
yuchie@nycu.edu.tw

¹ Department of Applied Chemistry, National Yang Ming Chiao Tung University, Hsinchu 300, Taiwan

² Department of Applied Mathematics, National Yang Ming Chiao Tung University, Hsinchu 300, Taiwan

³ Institute of Artificial Intelligence Innovation, National Yang Ming Chiao Tung University, Hsinchu 300, Taiwan

⁴ National Center for Theoretical Sciences, National Taiwan University, Taipei 10617, Taiwan

⁵ International College of Semiconductor Technology, National Yang Ming Chiao Tung University, Hsinchu 300, Taiwan

Introduction

Staphylococcus aureus has been ranked as the number one pathogen that causes the most deaths related to bacterial infections globally [1]. Generally, methicillin-resistant *S. aureus* (MRSA) strains are usually called superbugs, which have caused difficulties in treating patients infected with such pathogens [2]. Given that the antibiotics used to treat methicillin-sensitive *S. aureus* (MSSA) and MRSA are very different [3], it is vital to distinguish *S. aureus* from its drug-resistant strains. The standard methods that have been applied to test bacteria with drug-resistance are the bacterial culture-based methods—antimicrobial susceptibility testing, such as broth dilution and disk diffusion test [4]. These methods can provide the minimum inhibitory concentration (MIC) of different drugs against specific bacteria [5, 6]. However, they are time-consuming since overnight

culture is required. With the development of biotechnology, polymerase chain reaction (PCR) is an alternative method that can be used to distinguish different *S. aureus* strains [7]. PCR can amplify specific DNA sequences for different strains of *S. aureus*. However, it requires specific primers for target bacteria, takes a few hours to complete the analysis, and requires professional personnel to operate the instrument. Surface plasmon resonance has also been used to distinguish *S. aureus* [8]. Nevertheless, its experimental steps are complicated, including the requirements of conducting DNA extraction and PCR. Analytical methods that can be used to rapidly distinguish MRSA from MSSA are still in high demand.

Mass spectrometry (MS) has been used to characterize bacteria [9–17]. Bacteria can be identified based on their fingerprint mass spectra in terms of their protein or metabolite profiles [9–17]. Matrix-assisted laser desorption/ionization (MALDI)-MS [9–13, 15–17] has been extensively used to detect intact bacterial cells because of its simplicity and speed. Unlike PCR, MALDI mass spectra of intact bacterial cells can be obtained in a few minutes. Protein profiles derived from bacteria shown in the MALDI fingerprint mass spectra possess excellent distinguishing capability in the bacterial species levels. However, it is still a challenge to distinguish different strains of bacteria. Thus, to explore suitable strategies that can be used to solve this challenging issue is still necessary. One possible solution is principal component analysis (PCA), which has been used to classify bacteria with good identification capabilities [18, 19]. With the increasing reliability of machine learning technology, various supervised learning strategies, including support vector machines and random forests, have also been applied to differentiate bacteria at the strain level, achieving an accuracy of around 90% [20–27]. Nevertheless, efforts are still required to improve the identification power and reduce the analysis time.

Most studies stated above were focused on the examination of the bacteria obtained after overnight culture [20–27]. It would be desirable if the time spent on overnight culture could be eliminated or reduced when analyzing real-world samples. Thus, affinity methods that can be used to selectively enrich bacteria from sample solutions by eliminating overnight cultures have been developed [13, 15, 28]. Magnetic nanoparticles (MNPs) such as functional Fe_3O_4 MNPs [13, 15, 28] have been extensively used as affinity probes in the enrichment of trace bacteria from sample solutions owing to their magnetism for ease of isolation of MNP-bacterium conjugates. Bare Fe_3O_4 MNPs also exhibit affinity toward bacteria, which are rich in oxygen-containing functional groups. The interaction

between bare Fe_3O_4 MNPs and bacteria arises from the high affinity between Fe^{3+} on the MNPs and oxygen-containing functional groups (e.g., phosphates) on the bacterial surfaces according to the Hard Soft Acid Base theory [29]. Moreover, Fe_3O_4 MNPs are easy to prepare and synthesize [13, 15, 28], so they should be suitable probes for enrichment of bacteria from sample solutions for MALDI-MS analysis. In this study, we used Fe_3O_4 MNPs as affinity probes to enrich bacteria, followed by MALDI-MS analysis. To shorten the analysis time, microwave-heating [30–32] was used to accelerate the trapping of bacteria by the magnetic probes. The MS results were processed by using a machine-learning model. Our approach began with assembling a comprehensive dataset involving the MALDI spectra of four distinct *S. aureus* strains. We employ a neural network-based classification model to process the dataset. A distinctive feature of our data lies in its nature as a binary classification task, albeit with four labeled categories. Therefore, we employ the quaternary classification model for the training task and subsequently convert the model's prediction results into binary classification. The established dataset was utilized to examine whether the sample containing trace bacteria can be identified using this approach. Using Fe_3O_4 MNP-based probes against target bacteria under microwave-heating incubation can significantly reduce the analysis time from several hours to just a couple of minutes. The current approach can overcome the time-consuming overnight culture required for the preparation of bacterial samples. Additionally, it demonstrates the possibility of employing MNP-based enrichment of trace bacteria in real-world samples for rapid distinguishing between MRSA and MSSA.

Experimental section

Chemicals and reagents

Ferrous (II) chloride tetrahydrate, hydrochloric acid (36.5–38.0%), tris(hydroxymethyl) aminomethane (Tris), and Tris hydrochloride were purchased from J. T. Baker (Phillipsburg, NJ, USA). Acetonitrile, ammonium hydroxide solution (30 ~ 33%), α -cyano-4-hydroxycinnamic acid (CHCA), iron (III) trichloride hexahydrate, and trifluoroacetic acid (TFA) were purchased from Merck (Darmstadt, Germany), Fluka (Charlotte, NC, USA), Sigma-Aldrich (St. Louis, MO, USA), Alfa Aesar (Massachusetts, USA), and Duksan (Ansan, South Korea), respectively. Ethanol was purchased from Echo (Miaoli, Taiwan), whereas pure water was purchased from Taisun (Changhua, Taiwan). Tryptic soy broth (TSB) was

purchased from Himedia (Kennett Square, PA, USA). Yeast extract was purchased from Alpha Biosciences (Baltimore, MD, USA). *S. aureus* (an MSSA strain) and methicillin-resistant *S. aureus* (MRSA) were obtained from the Tzu-Chi Hospital (Hualien, Taiwan) and provided by Prof. P.-J. Tsai (NCKU, Taiwan). The other two MSSA strains, including *S. aureus* ATCC 6538DR (BCRC 10823) and *S. aureus* ATCC 12692 (BCRC 10831), were purchased from the Bioresource Collection Research Center (BCRC) (Hsinchu, Taiwan). Apple juice was purchased from a local shop.

Instrumentation

All the MALDI mass spectra were acquired from an Autoflex III MALDI-time of flight (TOF) mass spectrometer (Bruker Daltonics, Bremen, Germany). The mass spectrometer was equipped with a Nd:YAG laser with a wavelength of 355 nm. All the samples were conducted by the linear TOF with the positive ion mode. The voltages on the mass spectrometer were set as follows: ion source 1, 20.00 kV; ion source 2, 18.65 kV; lens, 6.80 kV. The laser frequency was set at 100 Hz. Bacteria were cultured in an incubator (Deng Yng DB60, Taipei, Taiwan) at 37 °C. The optical density of bacterial suspension at the wavelength of 600 nm (OD_{600}) was recorded using either a Biochrom WPA CO8000 (Cambridge, UK) or a Biosan DEN-600 Photometer (Riga, Latvia).

Bacterial culture

S. aureus (clinical, BCRC 10823, BCRC 10831, and MRSA clinical strains) were cultured on the agar plate containing TSB and yeast extract (TSBY) at 37 °C for ~20 h. TSBY agar plates were prepared by dissolving TSB (10 g), yeast extract (2 g), and agar (10 g) in deionized water (400 mL), followed by sterilization and pulling to individual Petri dishes. Freshly harvested bacteria were used for the experiments in the study.

MALDI-MS analysis of model bacteria

A couple of *S. aureus* colonies prepared above were mixed with TFA (3%, 20 μ L). The resulting bacterial sample (1.5 μ L) was mixed with the MALDI matrix (1.5 μ L), i.e., CHCA (25 mg mL⁻¹), which was prepared in acetonitrile/3% TFA (2:1, v/v). The resulting mixture (1.5 μ L) was deposited on the MALDI plate. After solvent evaporation, the sample was ready for MALDI-MS analysis, in which the linear TOF was

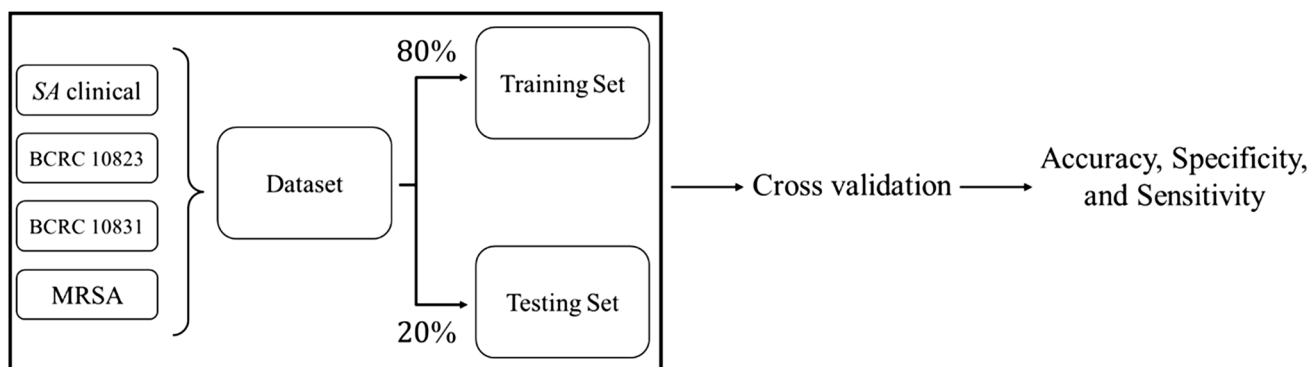
operated with the positive ion mode. The laser frequency was set at 100 Hz. Each mass spectrum acquired with the m/z range of 3000–8000 was collected from 3000 to 10,000 laser shots until the peak at m/z 6888 reaching the intensity of ~2000. 63, 52, 54, and 64 mass spectra derived from *S. aureus* clinical strain, *S. aureus* BCRC 10823, *S. aureus* BCRC 10831, and MRSA clinical strain, respectively, were acquired to establish the machine learning dataset.

Using a machine learning strategy to build a classification model for four model *S. aureus* strains

The classification model and deep SHAP analysis were implemented using the Python programming language. The machine learning model comprises three parts. The initial stage involves data preprocessing, followed by utilizing a neural network quaternary classification model in the second part. Lastly, the third component involves a post-processing binary classification model. The first and last parts are predefined and do not require training, while the classification model of the second part contains unknown parameters that need to be learned from the data. The details of the machine learning algorithm used to classify the four *S. aureus* based on our MALDI-MS data were provided in the Appendix I in Electronic Supporting Material (ESM).

Using Fe₃O₄ MNPs as affinity probes to trap model bacteria

The freshly harvested bacteria, as prepared above, were centrifuged at 6000 rpm for 3 min. The bacteria cells were rinsed with Tris buffer (5 mL, pH 6) and centrifuged at 6000 rpm for 3 min, repeating the process for two cycles. After the rinse, the bacterial cells were suspended in Tris buffer with an OD_{600} equal to 1. The bacterial suspension was further diluted to the desired concentrations before the experiments. Fe₃O₄ MNPs were generated based on the protocol reported previously [33]. The details of the preparation of Fe₃O₄ MNPs were provided in the Appendix II in ESM. When using Fe₃O₄ MNPs as affinity probes against the model bacteria, Fe₃O₄ MNPs (~50 μ g) were added to the sample (1 mL) containing *S. aureus*. The mixture was vortex-mixed for a few seconds and subjected to microwave-heating (power, 180 W) for 2 min. The resulting MNP-bacterium conjugates were magnetically isolated using an external magnet for approximately 5 min. The supernatant was then removed, TSBY (1 mL) was added, and the solution was incubated for another 4–6 h. After incubation, the remaining MNPs were discarded by magnetic isolation, whereas the remaining supernatant containing newly grown



Scheme 1 Schematic illustration of random data separating and testing process (SA stands for *S. aureus*)

bacteria was centrifuged at 6000 rpm for 5 min, followed by rinse with Tris buffer (20 mM, pH 6) for four cycles. After rinsing, a new batch of Fe_3O_4 MNP ($\sim 30 \mu\text{g}$) and Tris buffer (20 mM, $\sim 0.9 \text{ mL}$) were added to the rinsed bacterial cells to have a final volume of 1 mL. The mixture was vortex-mixed for a few seconds, followed by microwave-heating. The MNP-bacterium conjugates were magnetically isolated by placing an external magnet for 5 min to remove the supernatant, followed by centrifugation at 6000 rpm for 5 min, and the supernatant was discarded. The resulting MNP-bacterium conjugates were mixed with the MALDI matrix ($1.5 \mu\text{L}$). The MALDI matrix was prepared by dissolving CHCA (25 mg mL^{-1}) in acetonitrile/3% TFA (2:1, v/v). The resulting mixture was deposited on the well on the MALDI plate. After solvent evaporation, the sample was ready for MALDI-MS analysis.

Analysis of simulated real samples

Apple juice was used to prepare simulated real samples. That is, 100-fold diluted apple juice samples prepared in Tris buffer (20 mM, pH 6) were spiked with model bacteria with different concentrations. The experimental steps using Fe_3O_4 MNPs as affinity probes followed by MALDI-MS analysis

were similar to those steps stated above. The resulting mass spectral data were input to the established database using the developed machine-learning strategy.

Results and discussion

MALDI mass spectra of four model *S. aureus*

Four *S. aureus* strains, including one clinical strain, BCRC 10823, BCRC 10831, and one MRSA strain, were selected as the model bacteria in this study. The MIC of *S. aureus* against oxacillin has been used as the guideline to distinguish MSSA from MRSA [6]. The MICs of *S. aureus* clinical strain, BCRC 10823, BCRC 10831, and MRSA clinical strain toward oxacillin were 0.25, 0.25, 0.25, and $16 \mu\text{g mL}^{-1}$, respectively (ESM Figure S1), whereas they were <0.125 , 0.5, 0.5, and $2 \mu\text{g mL}^{-1}$, respectively, toward vancomycin (ESM Figure S2). That is, these four strains are vancomycin sensitive, whereas *S. aureus* clinical strain, BCRC 10823, and BCRC 10831 were confirmed as MSSA. Figure 1 shows the representative MALDI spectra of these four *S. aureus* strains obtained from the linear MALDI-TOF operated at the positive ion mode. The peaks at m/z 5032, 5525, and 6888 were observed in all the mass spectra of these four *S. aureus* strains. Given that the peak at m/z 6888 was the major peak among these bacterial strains, we acquired the MALDI mass spectra of individual samples

Table 1 Model confusion matrix of testing set for four model *S. aureus* strains. SA stands for *S. aureus*

	Clinical SA Predicted	SA 10823 Predicted	SA 10831 Predicted	MRSA Predicted	Accuracy (%)
Clinical SA	252	0	0	8	96.92
SA 10823	5	214	1	0	97.27
SA10831	7	7	203	3	92.27
MRSA	9	0	0	251	96.54

Table 2 Classification results for MSSA and MRSA

	MSSA predicted	MRSA predicted
MSSA	689 (a)	11 (b)
MRSA	9 (c)	251 (d)

Accuracy = $((a+d)/(a+b+c+d))\%$; Sensitivity = $(a/(a+b))\%$; Specificity = $(d/(c+d))\%$

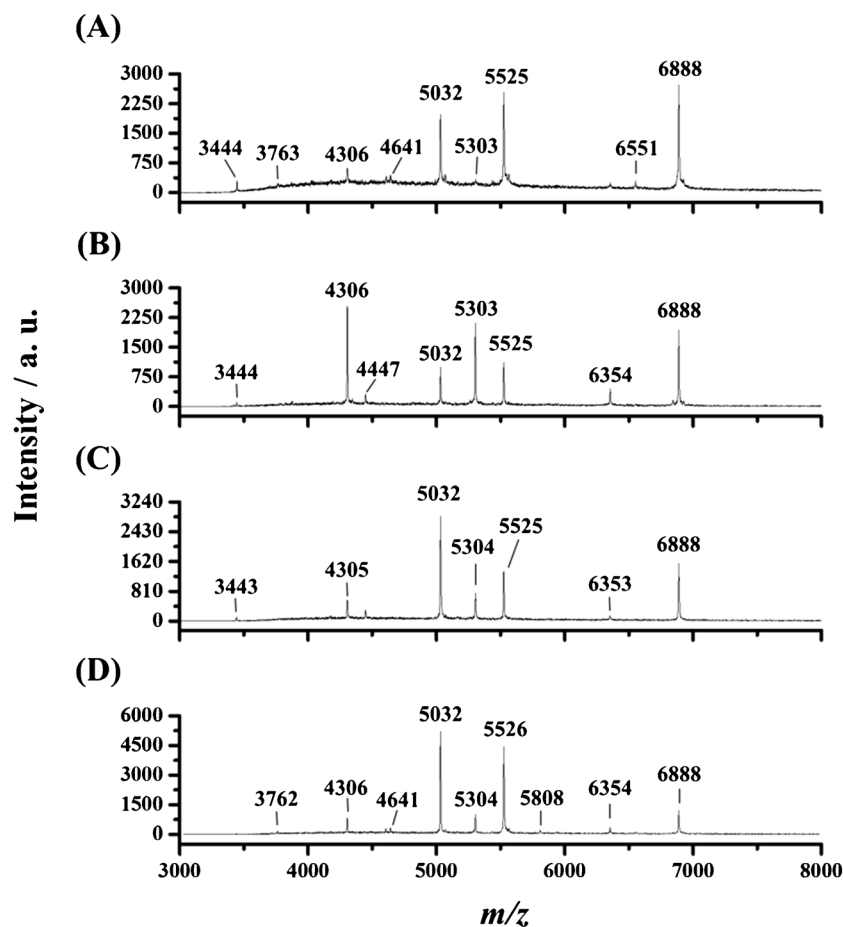
Table 3 Accuracy, sensitivity, and specificity in classifying MSSA and MRSA

	Accuracy	Sensitivity	Specificity
Test results	97.92%	98.43%	96.54%

Accuracy = $((a + d)/(a + b + c + d))\%$; Sensitivity = $(a/(a + b))\%$; Specificity = $(d/(c + d))\%$

with intensities of this peak up to ~2000 during MALDI-MS analysis. It should be noted that the mass resolution used in the linear mode was less than 2000. Consequently, the m/z values derived from the same peak may have a discrepancy of 1–3 amu. For example, the peak at m/z 5526 in Fig. 1D should be the same as the peak at m/z 5525 shown in Fig. 1A–C. The peak at m/z 4305 in Fig. 1C should be the same at m/z 4306 shown in Fig. 1A, B, and D. There was not a significant difference in mass spectral profiles among MSSA and MRSA strains. However, the relative intensity of ion peaks in the mass spectra varied among the strains. Therefore, we further employed a machine-learning strategy to investigate whether these different *S. aureus* strains could be distinguished from each other.

Fig. 1 Representative MALDI mass spectra of *S. aureus* **A** clinical ($n=63$), **B** BCRC 10823 ($n=52$), **C** BCRC 10831 ($n=54$), and **D** MRSA clinical strains ($n=64$). “ n ” stands for the number of the mass spectra of the individual bacterial strains that were acquired. One or two *S. aureus* colonies were mixed with 3% TFA (20 μ L). The resulting bacterial sample (1.5 μ L) was then mixed with the MALDI matrix CHCA (25 mg mL⁻¹), prepared in acetonitrile/3% TFA (2:1, v/v). This mixture (1.5 μ L) was deposited onto the MALDI plate. After solvent evaporation, the sample was ready for MALDI-MS analysis using the linear TOF in positive ion mode



Neural network-based classification model for *S. aureus* strains

The total number of the MALDI spectra derived from those four *S. aureus* strains was 233. Scheme 1 shows the schematic illustration to describe how the data was selected and processed in the classification model. We used cross-validation to check the accuracy of the model.

The model was trained 20 times. At each time, the data was divided into training and test sets. We randomly selected 80% of the MALDI spectra as the training dataset, while the remaining 20% constituted the test dataset. A classification model was trained using training data, whereas accuracy, sensitivity, and specificity were calculated using test data. The final performance metrics are averaged over the 20 iterations.

Table 1 indicates that the accuracy for identifying four *S. aureus* strains, including clinical strains BCRC 10823 and BCRC 10831, as well as the MRSA clinical strain, was 96.92%, 97.27%, 92.27%, and 96.54%, respectively. In Table 2, MSSA and MRSA were classified by placing *S. aureus* clinical strains BCRC 10823 and BCRC 10831 in the MSSA group. Table 3 presents the resulting accuracy, sensitivity, and specificity as 97.92%, 98.43%, and 96.54%, respectively, based on the outcomes listed

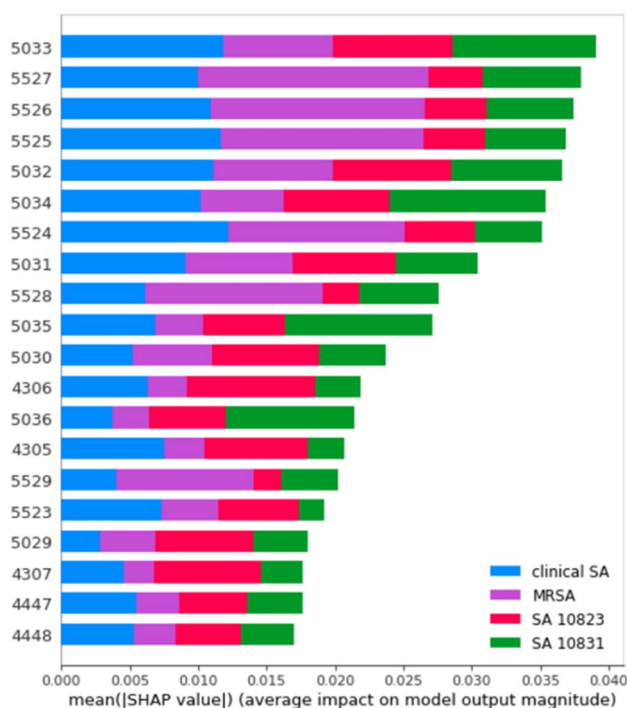


Fig. 2 Mean absolute SHAP values in Deep SHAP results obtained from the MALDI mass spectra of four model bacterial strains. The sample preparation steps were stated in the legend shown in Fig. 1

in Table 2. These findings demonstrate that the model effectively predicts the target strains using the established dataset. Furthermore, the machine-learning strategy achieved high accuracy, sensitivity, and specificity in classifying MSSA and MRSA.

Characterization of the feature peaks

To determine the feature peaks in each strain, we used Deep SHapley Additive exPlanations (SHAP) to characterize the important peaks in the mass spectrum of each strain. Figure 2 shows the essential features found by Deep SHAP and the influence of these feature peaks on each strain. Figure 3 shows the model SHAP value impact on model output for each strain. The top five feature peaks in each strain are listed below: the feature peaks for clinical strain were m/z 5524, 5033, 5525, 5032, and 5526; for BCRC 10823 were m/z 4306, 5033, 5032, 4307, and 5030; for BCRC 10831 were m/z 5034, 5035, 5033, 5036, and 5032; and for MRSA strain were m/z 5527, 5526, 5525, 5524, and 5528. Let us take Figure 3A as an example; the figure classified the data into two groups: one is the target group, i.e., MRSA, listed on the positive coordinates; the other one is the non-target group (clinical, BCRC 10823 and BCRC 10831) listed on the negative coordinates. The red spots denoted the feature having a significant influence in this group, whereas the blue spots denoted the feature having a low influence. The top five features in Fig. 3A were m/z 5527,

5526, 5525, 5524, and 5528, derived from MRSA, which were marked with red spots at the positive coordinates. Given that we operated the MALDI mass spectrometer at the linear mode when analyzing these model bacteria, as mentioned earlier, the mass resolution was not good, resulting in the broad peak observed in Fig. 1. Thus, these discovered feature peaks were, in fact, derived from the same identity. That is, the feature peak at m/z 5525 standing for MRSA. The feature peak of *S. aureus* BCRC 10831, as shown in Fig. 3B, was m/z 5033 (m/z 5033 ± 2). In Fig. 3C for *S. aureus* BCRC 10823, two feature peaks were apparent at m/z 4306 (i.e., m/z 4306 and 4307) and m/z 5033 (i.e., m/z 5033, 5032, and 5030). Notably, the presence of red color spots at m/z 4306 and blue color spots at m/z 5033 in BCRC 10823 implies a more pronounced influence of the feature peaks at m/z 4306 and a comparatively lesser influence of those at m/z 5033. Examining the *S. aureus* clinical strain depicted in Fig. 3D, Deep SHAP analysis revealed multiple characteristic peaks. However, a distinctive pattern emerges: all of these features exhibit blue color spots on positive coordinates. This outcome signifies that the machine learning model initially identifies spectra resembling MRSA, BCRC 10831, and BCRC 10823. That is, those discovered ions have a low influence in identifying the *S. aureus* clinical strain. Should the spectra fail to align with these three strains, the model subsequently classifies them as belonging to the *S. aureus* clinical strain. These feature peaks enabled the classification model to distinguish different model strains.

Using Fe_3O_4 MNPs as affinity probes to trap model bacteria

We further examined the possibility of using Fe_3O_4 MNPs as affinity probes to enrich target bacteria in the sample solution. Therefore, the time for overnight culture could be eliminated. The details of the experimental steps have been provided in the “Experimental section.” ESM Table S1 shows the binding capacity of Fe_3O_4 MNPs against *S. aureus* clinical strain at different pH values. The result shows that with the increase of the pH value, the binding capacity of the MNPs toward *S. aureus* was reduced. The optimal binding capacity appeared at pH 5 and 6.

Figure 4A, B, and C show the MALDI mass spectra of MRSA clinical strain with the concentrations of OD values of 10^{-1} , 10^{-2} , and 10^{-3} , respectively, from direct MS analysis. It was apparent that no peaks were found in the mass spectra. After MNP enrichment from the sample (1 mL) containing MRSA clinical strain with the concentrations of OD values of 10^{-1} and 10^{-2} , the peaks representing the target bacteria could be observed in the mass spectra (Fig. 4D and E). However, it was impossible to see any peaks when the concentration of the target bacteria was lowered to OD of 10^{-3} (Fig. 4F).

To further improve the lowest detectable concentration, we cultured the bacteria trapped on the MNPs for 6 h before

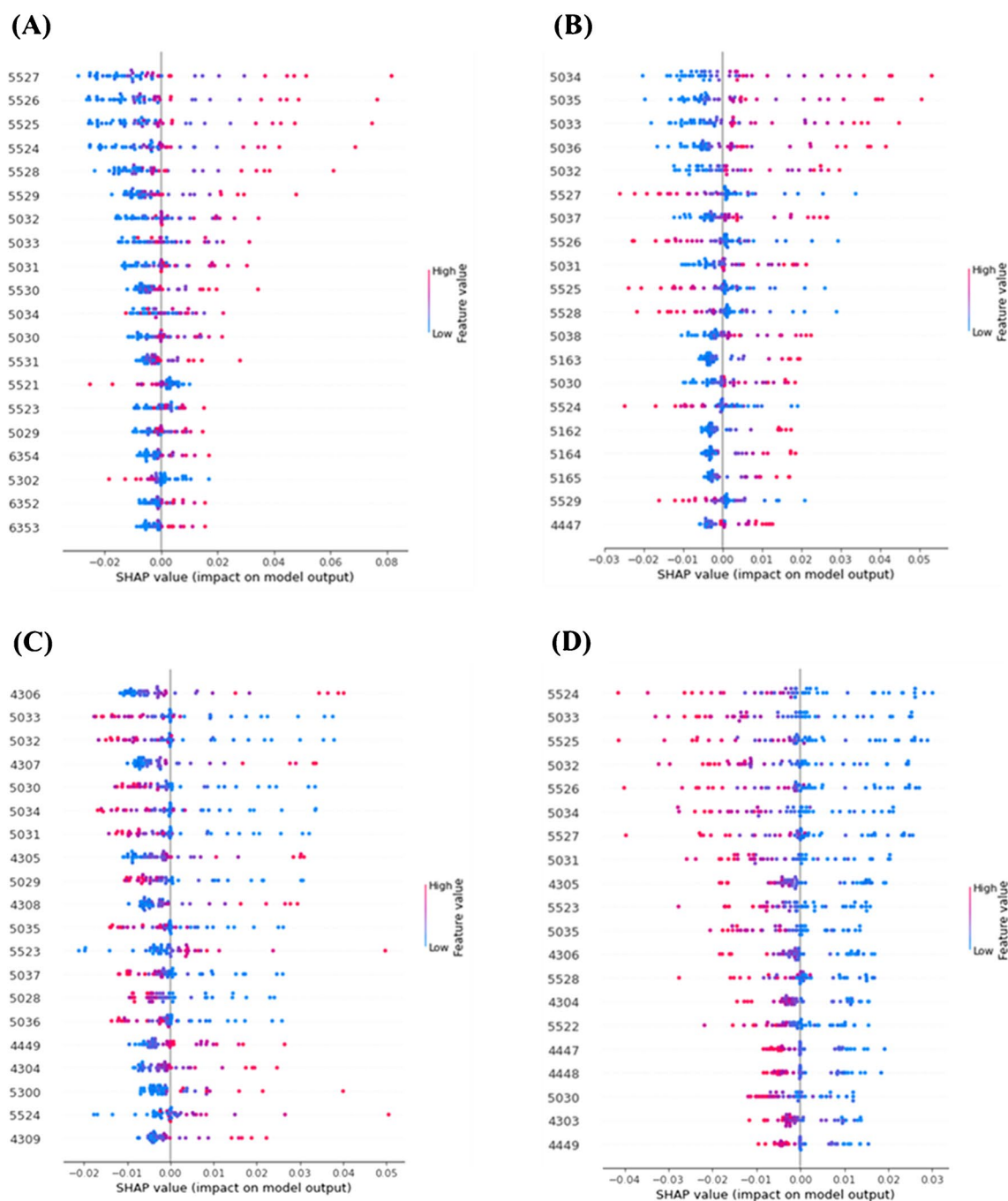


Fig. 3 SHAP values that impact on model output for the direct MALDI mass spectra obtained from the samples containing **A** MRSA clinical strain ($n=64$), **B** *S. aureus* BCRC 10831 ($n=54$), **C** *S.*

aureus BCRC 10823 ($n=52$), and **D** *S. aureus* clinical strain ($n=63$). The sample preparation steps were stated in the legend shown in Fig. 1

MALDI-MS analysis. The detailed experiment steps were described in the “Experimental section.” MRSA clinical strain was used as the model bacteria. Figure 5 shows the resultant mass spectra of the sample containing MRSA clinical strain with different concentrations in terms of OD values of 10^{-7} – 10^{-4} obtained after using Fe_3O_4 MNPs as affinity probes for enrichment, followed by 6-h culture. Those

peaks marked with red m/z values were derived from MRSA. Apparently, the peaks representing the MRSA appeared in the mass spectra as the concentration of the target bacterium was reduced to the OD of 10^{-5} . As the concentration of the target bacterium was reduced to 10^{-6} , only one peak at m/z 4307 derived from the MRSA clinical strain was observed in the mass spectrum. ESM Table S2 shows the classification

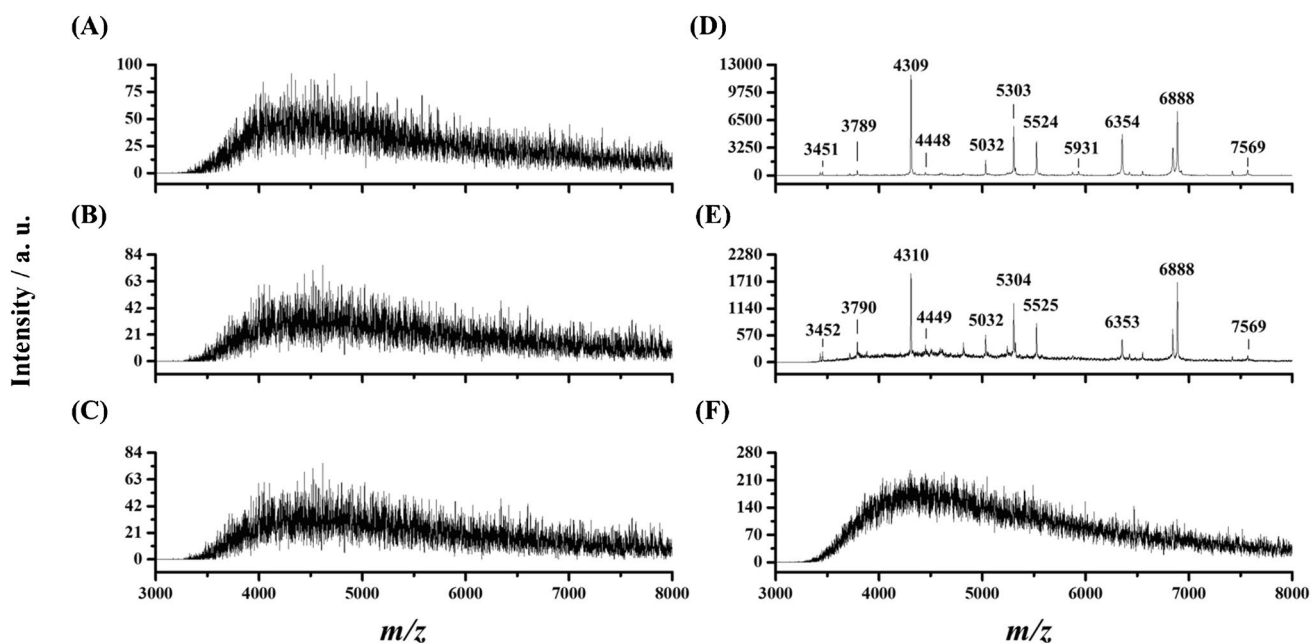


Fig. 4 Direct MALDI mass spectra of MRSA clinical strain with the concentrations in terms of OD values of **A** 10^{-1} , **B** 10^{-2} , and **C** 10^{-3} . MALDI mass spectra of the same bacterial samples (1 mL) with the concentrations of OD values of **D** 10^{-1} , **E** 10^{-2} , and **F** 10^{-3} obtained

after using Fe_3O_4 MNPs (50 μg) to enrich trace target bacteria from the samples followed by MALDI-MS analysis. The samples were incubated under microwave heating for the MNP enrichment

Fig. 5 MALDI mass spectra of the samples (1 mL) containing MRSA clinical strain with the concentrations in terms of the OD values of **A** 10^{-4} , **B** 10^{-5} , **C** 10^{-6} , and **D** 10^{-7} obtained after enriched by Fe_3O_4 MNPs (50 μg) under microwave-heating followed by 6-h culture

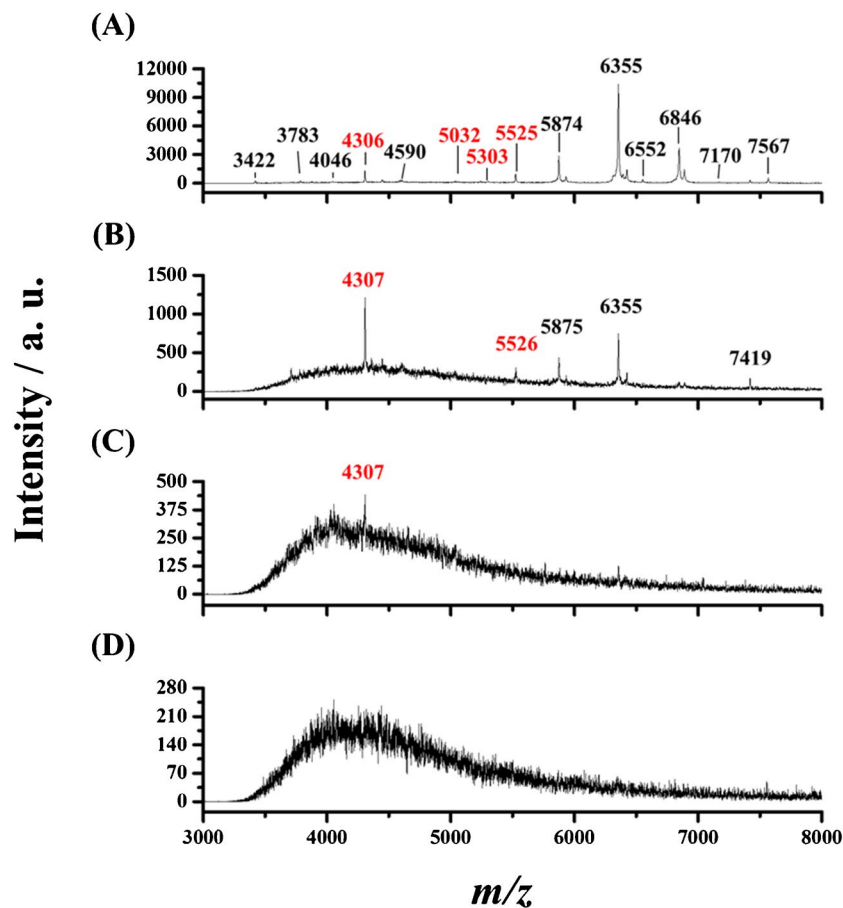
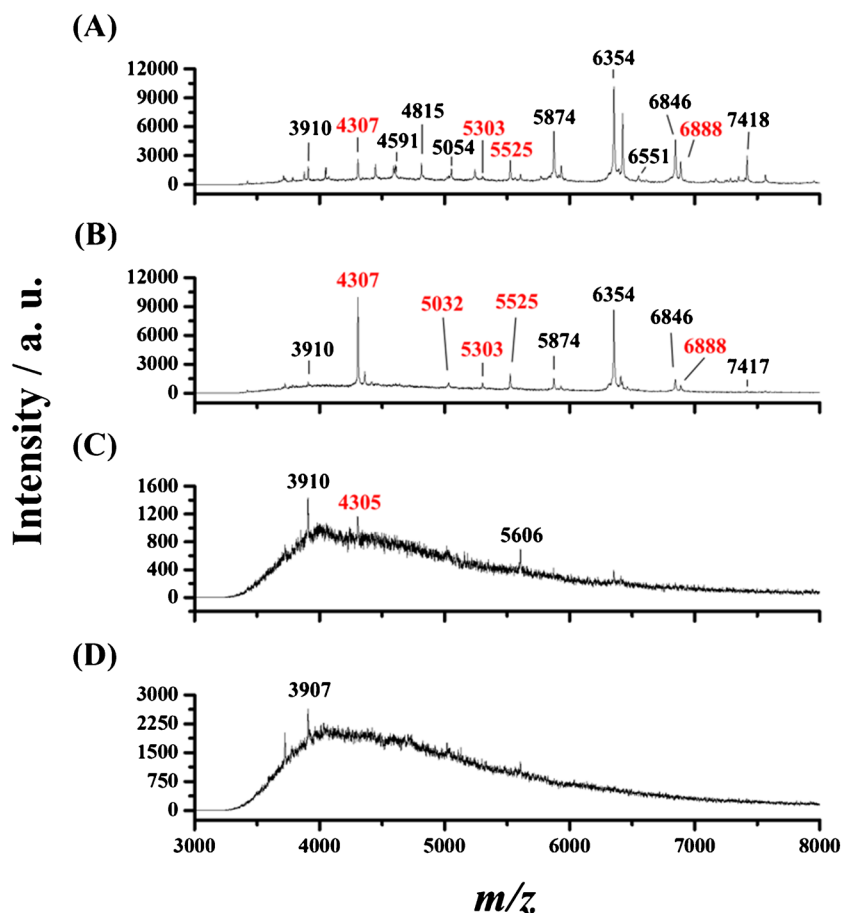


Fig. 6 MALDI mass spectra of the 100-fold diluted juice samples (1 mL) containing MRSA clinical strain with the concentrations in terms of the OD values of **A** 10^{-4} , **B** 10^{-5} , **C** 10^{-6} , and **D** 10^{-7} obtained after enriched by Fe_3O_4 MNPs (50 μg) under microwave-heating followed by 6-h culture. The peaks marked with red text were derived from MRSA



result. When the samples containing MRSA have concentrations in terms of OD values of 10^{-4} and 10^{-5} , the established model can correctly identify the target bacteria, i.e., MRSA. However, the model failed to identify the target bacteria as the bacterial concentration was further reduced to the OD value of 10^{-6} . It was because many feature peaks appeared in the resulting mass spectra of the samples containing the target bacteria with a high concentration, whereas few peaks were observed in the resulting mass spectra of the samples containing a low concentration of target bacteria. These results indicated that the lowest detectable concentration of MRSA clinical strain could be reduced to the concentration with the OD value of $\sim 10^{-5}$ ($\sim 4 \times 10^4$ CFU mL^{-1}) after enrichment, followed by a 6-h culture. The detection limit of the approach was estimated to be approximately $\sim 8 \times 10^3$ CFU mL^{-1} (OD of 1 = $\sim 4 \times 10^9$ CFU mL^{-1}) [34] by considering the peak at m/z 4307 (a signal-to-noise ratio (S/N) of 15), representing MRSA (Fig. 5B, the concentration of MRSA = OD of $\sim 10^{-5}$) based on an S/N of 3.

Real sample analysis

We then examined the feasibility of using the developed method to characterize target bacteria in the simulated real

sample. A 100-fold diluted apple juice by Tris buffer (pH 6) was spiked with MRSA clinical strain with different concentrations and treated by our developed method, the same as that used to obtain Fig. 5. Figure 6 shows the resulting MALDI mass spectra. Many feature peaks, including m/z 4307, 5032, 5303, 5524, 5525, and 6888 (marked in red) that were discovered by DEEP SHAP, were observed (Fig. 3). The data obtained in Fig. 6 were processed using the established dataset based on the developed machine learning model. ESM Table S3 shows the machine learning results for identifying target bacteria using the established machine learning model. The identity of the target bacteria could be correctly identified even though the concentration of MRSA clinical strain was reduced to the OD value of 10^{-5} . The results indicated the potential of using the developed method to analyze target bacteria in complex samples.

Comparison of our approach with the existing methods

ESM Table S4 shows a list comparing the existing methods [21, 23–26, 35–37] with our approach. Although our method required a 6-h incubation time after MNP enrichment, all the existing methods [21, 23–26, 35–37] required 12–24 h

before MALDI-MS analysis could be carried out. That is, MNP enrichment can be used to effectively reduce the entire time for sample preparation. Nevertheless, the current method still requires a 6-h culture for the bacterial samples with their $OD < \sim 10^{-2}$ ($\approx 10^7$ CFU mL⁻¹) (cf. Figure 4 and Fig. 5), to obtain sufficient bacterial cells for MALDI-MS analysis and correct identifications by our machine learning strategy. Thus, further efforts should be devoted to the reduction of the sample preparation time. Moreover, our method has a relatively low LOD, i.e. $\sim 8 \times 10^3$ CFU mL⁻¹ compared with the existing methods [21, 23–26, 35–37]. The accuracy of our method was 92–97%, which was relatively good, compared with most of the existing methods [21, 23–26, 35, 36].

Conclusions

Machine-learning strategies have been used to effectively distinguish different bacteria based on the MALDI mass spectra of intact bacterial cells. Nevertheless, time-consuming overnight culture is usually required prior to MS analysis. In this study, we have developed a method that combines affinity based-MS with a machine-learning strategy to distinguish MRSA from MSSA. Fe₃O₄ MNPs were demonstrated to be useful affinity probes that could be used to effectively enrich trace bacteria from the sample solution within 2 min under microwave-heating. Therefore, overnight culture time could be further reduced to 6 h for correctly identifying trace bacteria from the sample solution. Our machine-learning model demonstrated commendable classification prowess, yielding high accuracy levels for each *S. aureus* strain. We found distinctive feature peaks associated with each strain using the Deep SHAP methodology. Based on our results, the developed Fe₃O₄ MNP-based affinity MALDI-MS combined with a deep learning strategy provides a new method to effectively reduce the entire analysis time, which is the main advantage over the existing methods. Enrichment of target bacteria with the concentration $\geq \sim 10^7$ CFU mL⁻¹ followed by MALDI-MS analysis can be completed within 10 min. However, the current method still requires 6-h culture for the bacteria samples with the concentration lower than 10^7 CFU mL⁻¹ to obtain enough cells for MALDI-MS analysis and accurate identifications with our machine learning strategy. Thus, efforts are still needed to further reduce the time in the sample preparation. Therefore, it will be possible for on-site detection of pathogenic bacteria.

Supplementary Information The online version contains supplementary material available at <https://doi.org/10.1007/s00604-024-06342-z>.

Funding Open Access funding enabled and organized by National Yang Ming Chiao Tung University This study is financially

supported by the National Science and Technology Council, Taiwan (111–2113-M-A49-019-MY3 and 111–2628-M-A49-008-MY4).

Declarations

Conflict of interest The authors declare no competing interests.

Open Access This article is licensed under a Creative Commons Attribution 4.0 International License, which permits use, sharing, adaptation, distribution and reproduction in any medium or format, as long as you give appropriate credit to the original author(s) and the source, provide a link to the Creative Commons licence, and indicate if changes were made. The images or other third party material in this article are included in the article's Creative Commons licence, unless indicated otherwise in a credit line to the material. If material is not included in the article's Creative Commons licence and your intended use is not permitted by statutory regulation or exceeds the permitted use, you will need to obtain permission directly from the copyright holder. To view a copy of this licence, visit <http://creativecommons.org/licenses/by/4.0/>.

References

- Ikuta KS, Swetschinski LR, Aguilar GR, Sharara F, Mestrovic T, Gray AP, Weaver ND, Wool EE, Han C, Hayoon AG (2022) Global mortality associated with 33 bacterial pathogens in 2019: a systematic analysis for the Global Burden of Disease Study 2019. *Lancet* 400:2221–2248
- Gordon RJ, Lowy FD (2008) Pathogenesis of Methicillin-resistant *Staphylococcus aureus* infection. *Clin Infect Dis* 46(Supplement_5):S350–S359
- Boucher H, Miller LG, Razonable RR (2010) Serious infections caused by methicillin-resistant *Staphylococcus aureus*. *Clin Infect Dis* 51:S183–S197
- Reller LB, Weinstein M, Jorgensen JH, Ferraro MJ (2009) Antimicrobial susceptibility testing: a review of general principles and contemporary practices. *Clin Infect Dis* 49:1749–1755
- Wang G, Hindler JF, Ward KW, Bruckner DA (2006) Increased vancomycin MICs for *Staphylococcus aureus* clinical isolates from a university hospital during a 5-year period. *J Clin Microbiol* 44:3883–3886
- Broekema NM, Van TT, Monson TA, Marshall SA, Warshauer DM (2009) Comparison of cefoxitin and oxacillin disk diffusion methods for detection of mecA-mediated resistance in *Staphylococcus aureus* in a large-scale study. *J Clin Microbiol* 47:217–219
- van Hal SJ, Stark D, Lockwood B, Marriott D, Harkness J (2007) Methicillin-resistant *Staphylococcus aureus* (MRSA) detection: comparison of two molecular methods (IDI-MRSA PCR assay and genotype MRSA direct PCR assay) with three selective MRSA agars (MRSA ID, MRSA, and CHROMagar MRSA) for use with infection-control swabs. *J Clin Microbiol* 45:2486–2490
- Tawil N, Mouawad F, Lévesque S, Sacher E, Mandeville R, Meunier M (2013) The differential detection of methicillin-resistant, methicillin-susceptible and borderline oxacillin-resistant *Staphylococcus aureus* by surface plasmon resonance. *Biosens Bioelectron* 49:334–340
- Holland R, Wilkes J, Rafii F, Sutherland J, Persons C, Voorhees K, Lay J Jr (1996) Rapid identification of intact whole bacteria based on spectral patterns using matrix-assisted laser desorption/ionization with time-of-flight mass spectrometry. *Rapid Commun Mass Spectrom* 10:1227–1232

10. Ho Y-P, Reddy PM (2010) Identification of pathogens by mass spectrometry. *Clin Chem* 56:525–536
11. Chong BE, Wall DB, Lubman DM, Flynn SJ (1997) Rapid profiling of *E. coli* proteins up to 500 kDa from whole cell lysates using matrix-assisted laser desorption/ionization time-of-flight mass spectrometry. *Rapid Commun Mass Spectrom* 11:1900–1908
12. Demirev PA, Ho Y-P, Ryzhov V, Fenselau C (1999) Microorganism identification by mass spectrometry and protein database searches. *Anal Chem* 71:2732–2738
13. Chen W-J, Tsai P-J, Chen Y-C (2008) Functional nanoparticle-based proteomic strategies for characterization of pathogenic bacteria. *Anal Chem* 80:9612–9621
14. Basile F, Beverly MB, Voorhees KJ, Hadfield TL (1998) Pathogenic bacteria: their detection and differentiation by rapid lipid profiling with pyrolysis mass spectrometry. *TrAC Trends Anal Chem* 17:95–109
15. Lin Y-S, Tsai P-J, Weng M-F, Chen Y-C (2005) Affinity capture using vancomycin-bound magnetic nanoparticles for the MALDI-MS analysis of bacteria. *Anal Chem* 77:1753–1760
16. Ashfaq MY, Da'na DA, Al-Ghouti MA (2002) Application of MALDI-TOF MS for identification of environmental bacteria: a review. *J Environ Manage* 305:114359
17. Popović NT, Kazazić SP, Bojanić S-P, Čož-Rakovac R (2023) Sample preparation and culture condition effects on MALDI-TOF MS identification of bacteria: a review. *Mass Spectrom Rev* 42:1589–1603
18. Yan W, Qian J, Ge Y, Ye K, Zhou C, Zhang H (2020) Principal component analysis of MALDI-TOF MS of whole-cell foodborne pathogenic bacteria. *Anal Chem* 592:113582
19. Boots A, Smolinska A, Van Berkel J, Fijten R, Stobberingh E, Boumans M, Moonen E, Wouters E, Dallinga J, van Schooten F (2014) Identification of microorganisms based on headspace analysis of volatile organic compounds by gas chromatography–mass spectrometry. *J Breath Res* 8:027106
20. Weis CV, Jutzeler CR, Borgwardt K (2020) Machine learning for microbial identification and antimicrobial susceptibility testing on MALDI-TOF mass spectra: a systematic review. *Clin Microbiol Infect* 26:1310–1317
21. Bright JJ, Claydon MA, Soufian M, Gordon DB (2020) Rapid typing of bacteria using matrix-assisted laser desorption ionisation time-of-flight mass spectrometry and pattern recognition software. *J Microbiol Methods* 48:127–138
22. Khot PD, Couturier MR, Wilson A, Croft A, Fisher MA (2012) Optimization of matrix-assisted laser desorption ionization–time of flight mass spectrometry analysis for bacterial identification. *J Clin Microbiol* 50:3845–3852
23. Khot PD, Fisher MA (2013) Novel approach for differentiating *Shigella* species and *Escherichia coli* by matrix-assisted laser desorption ionization–time of flight mass spectrometry. *J Clin Microbiol* 51:3711–3716
24. Yu J, Tien N, Liu Y-C, Cho D-Y, Chen J-W, Tsai Y-T, Huang Y-C, Chao H-J, Chen C-J (2022) Rapid identification of methicillin-resistant *Staphylococcus aureus* using MALDI-TOF MS and machine learning from over 20,000 clinical isolates. *Microbiol Spectrum* 10:e00483-e522
25. Liu X, Su T, Hsu YMS, Yu H, Yang HS, Jiang L, Zhao Z (2021) Rapid identification and discrimination of methicillin-resistant *Staphylococcus aureus* strains via matrix-assisted laser desorption/ionization time-of-flight mass spectrometry. *Rapid Commun Mass Spectrom* 35:e8972
26. Wang H-Y, Chung C-R, Wang Z, Li S, Chu B-Y, Horng J-T, Lu J-J, Lee T-Y (2021) A large-scale investigation and identification of methicillin-resistant *Staphylococcus aureus* based on peaks binning of matrix-assisted laser desorption ionization-time of flight MS spectra. *Brief Bioinform* 22:bbaa138
27. Mortier T, Wieme AD, Vandamme P, Waegeman W (2021) Bacterial species identification using MALDI-TOF mass spectrometry and machine learning techniques: a large-scale benchmarking study. *Comput Struct Biotechnol J* 19:6157–6168
28. Bai Y-L, Shahed-Al-Mahmud M, Selvaprakash K, Lin N-T, Chen Y-C (2019) Tail fiber protein-immobilized magnetic nanoparticle-based affinity approaches for detection of *Acinetobacter baumannii*. *Anal Chem* 91:10335–10342
29. Pearson RG (1963) Hard and soft acids and bases. *J Am Chem Soc* 85:3533–3539
30. Chen W-Y, Chen Y-C (2007) Acceleration of microwave-assisted enzymatic digestion reactions by magnetite beads. *Anal Chem* 79:2394–2401
31. Chen W-Y, Chen Y-C (2007) MALDI MS analysis of oligonucleotides: desalting by functional magnetite beads using microwave-assisted extraction. *Anal Chem* 79:8061–8066
32. Lin S-S, Wu C-H, Sun M-C, Sun C-M, Ho Y-P (2005) Microwave-assisted enzyme-catalyzed reactions in various solvent systems. *J Am Soc Mass Spectrom* 16:581–588
33. Chen C-T, Chen Y-C (2005) Fe₃O₄/TiO₂ core/shell nanoparticles as affinity probes for the analysis of phosphopeptides using TiO₂ surface-assisted laser desorption/ionization mass spectrometry. *Anal Chem* 77:5912–5919
34. Jannatin M, Yang T-L, Su Y-Y, Mai R-T, Chen YC (2024) Europium Ion-Based Magnetic-Trapping and Fluorescence-Sensing Method for Detection of Pathogenic Bacteria. *Anal Chem*. <https://doi.org/10.1021/acs.analchem.4c00655>
35. Tang W, Ranganathan N, Shahrezaei V, Larrouy-Maumus G (2019) MALDI-TOF mass spectrometry on intact bacteria combined with a refined analysis framework allows accurate classification of MSSA and MRSA. *PLoS ONE* 14:e0218951
36. Kong P-H, Chiang C-H, Lin T-C, Kuo S-C, Li C-F, Hsiung C-A, Shiue Y-L, Chiou H-Y, Wu L-C, Tsou H-H (2022) Discrimination of methicillin-resistant *Staphylococcus aureus* by MALDI-TOF mass spectrometry with machine learning techniques in patients with *Staphylococcus aureus* bacteremia. *Pathogens* 11:586
37. Ciloglu FU, Caliskan A, Saridag AM, Kilic IH, Tokmakci M, Kahraman M, Aydin O (2021) Drug-resistant *Staphylococcus aureus* bacteria detection by combining surface-enhanced Raman spectroscopy (SERS) and deep learning techniques. *Sci Rep* 11:18444

Publisher's Note Springer Nature remains neutral with regard to jurisdictional claims in published maps and institutional affiliations.

Electronic Supporting Material

Distinguishing Methicillin-resistant *Staphylococcus aureus* from Methicillin-sensitive Strains by Combining Fe₃O₄ Magnetic Nanoparticle-based Affinity Mass Spectrometry with A Machine Learning Strategy

Wei-Hsiang Ma,^{1#} Che-Chia Chang,^{2,3#} Te-Sheng Lin,^{2,4*} Yu-Chie Chen^{1,5*}

¹Department of Applied Chemistry, National Yang Ming Chiao Tung University, Hsinchu 300, Taiwan

²Department of Applied Mathematics, National Yang Ming Chiao Tung University, Hsinchu 300, Taiwan

³Institute of Artificial Intelligence Innovation, National Yang Ming Chiao Tung University, Hsinchu 300, Taiwan

⁴National Center for Theoretical Sciences, National Taiwan University, Taipei 10617, Taiwan

⁵International College of Semiconductor Technology, National Yang Ming Chiao Tung University, Hsinchu 300, Taiwan

[#]The authors contributed equally to this work.

*Corresponding authors

T.-S. Lin

E-mail: teshenglin@nycu.edu.tw

Tel: +886-3-5712121 ext: 56422

Y.-C. Chen

E-mail: yuchie@nycu.edu.tw

Tel: +886-3-5131527

Fax: +886-3-5723764

Appendix I

1. Appendix – Neural network-based classification model

1.1. Data preprocessing

In the first stage, we aimed to normalize the mass spectrum intensity data for each *S. aureus* and extract representative values. The intensity of each data was normalized to one, and a max-pooling process was performed to obtain integer intensity between 3000 and 8000.

1.2. Multiclass classification model

We used a feedforward fully-connected neural network as the model. The dimension of the input layer is 5001, which is consistent with the number of input intensities. The output layer has four units to implement quaternary classification. At the last layer, the results are passed into a softmax function to obtain positive values with sum one, and the output class is the one with the most significant magnitude.

For model training, we utilize the conventional cross-entropy loss function and employ the Adam optimizer.

1.3. Binary classification model

To obtain a binary classification model, we added a layer to the output of the trained quaternary classification model. This layer does not require training, and its purpose is simply to condense quaternary classification into binary classification.

1.4. Validation

We used cross-validation to verify the robustness of the model. In each experiment, we randomly selected 80% of the data as the training set and the remaining 20% as the test set. The final accuracy of our model is the average of 20 experiments.

1.5. Feature importance

We used Deep SHAP [Lundberg, Scott M and Lee, Su-In, A Unified Approach to Interpreting Model Predictions, NIPS (2017), pp.4765–4774] to analyze the model and to find the important features. In the deep SHAP analysis, the mean absolute SHAP value illustrates the importance of each feature, and the sign of the SHAP value signifies which class the feature is most crucial for.

Appendix II

Additional Experimental Details

Synthesis of Fe₃O₄ MNPs

Iron (II) chloride (0.49 g) and iron (III) chloride (0.67 g) were initially dissolved in deionized water (25 mL) in a double-necked flask. The air in the double-necked flask was pumped out, followed by putting a balloon filled with nitrogen gas on one neck. Aqueous ammonia (33%, 25 mL) was slowly injected into the flask from the other sealed neck using a syringe connected to a syringe pump with a flow rate of 0.4 mL min⁻¹. The solution in the flask was continuously stirred at room temperature for 2 h, with all processes carried out under nitrogen protection. The generated Fe₃O₄ MNPs were aggregated on the wall of the vial using an external magnet (~4000 Gauss). The supernatant was then removed. The resulting Fe₃O₄ MNPs were washed with deionized water (20 mL × 1) and ethanol (20 mL × 3). Subsequently, the MNPs were suspended in ethanol (40 mL) and stored in a refrigerator at 4 °C until use.

Table S1. The binding capacity of Fe₃O₄ MNPs toward the *S. aureus* at different pH values.

pH value	5	6	7	8	9
Binding capacity (CFU mg ⁻¹)	$\sim 1.38 \times 10^{10}$	$\sim 1.38 \times 10^{10}$	$\sim 1.2 \times 10^{10}$	$\sim 1.08 \times 10^{10}$	$\sim 7.2 \times 10^9$

Table S2. Classification of the target bacteria using our machine learning strategy. “O” denotes that data was hit on the right one, whereas “X” indicates that the results were incorrect.

Samples	Results
MRSA (OD 10 ⁻⁴)	O
MRSA (OD 10 ⁻⁵)	O
MRSA (OD 10 ⁻⁶)	X
MRSA (OD 10 ⁻⁷)	X

Table S3. Identification of the target bacteria from the simulated real sample using our machine learning strategy. “O” denotes that the data was hit on the right one, whereas “X” indicated that the results were incorrect.

Samples	Results
MRSA (OD 10 ⁻⁴)	O
MRSA (OD 10 ⁻⁵)	O
MRSA (OD 10 ⁻⁶)	X
MRSA (OD 10 ⁻⁷)	X

Table S4. List of comparisons between the current work and the existing studies.

Reference number	Published Year	Target bacteria	Bacterial culture time	LODs	Number of mass spectra used in machine learning	Machine learning strategies	Accuracy
1	2002	35 different strains bacteria	24 h	-	212	Hybrid neural network	79% - 89%
2	2013	<i>Shigella</i> species/ <i>E. coli</i>	18-24 h	-	138	Genetic algorithm	90% - 96%
3	2019	MRSA/MSSA	12 h	$\sim 10^4$ cells μL^{-1} (= $\sim 10^7$ CFU mL^{-1})	140	BinDA, random forest	63% - 93%
4	2020	MRSA/MSSA	18-24 h	-	4858	Decision tree, random forest, Knearest Neighbor, and support vector machine	69.8% - 76.64%
5	2021	MRSA/MSSA	*-	-	548	Decision tree, polynomial regression, random forest, support vector machine	75% - 87%
6	2021	MRSA/MSSA	24 h	-	452	Support vector machine, random forest	82% - 86%
7	2022	MRSA/MSSA	24 h	-	33975	Deep neural network	$97.66 \pm 0.26\%$
8	2022	MRSA/MSSA	18-24 h	-	20359	LightGBM	**with AUC 0.78-0.88
This work	2023	MRSA/MSSA	6 h (after MNP capture)	$\sim 8 \times 10^3$ CFU mL^{-1}	233	Neural network	92% - 97%

* Not specified.

** This paper provides AUC, true positive rate, and true negative rate, instead of accuracy.

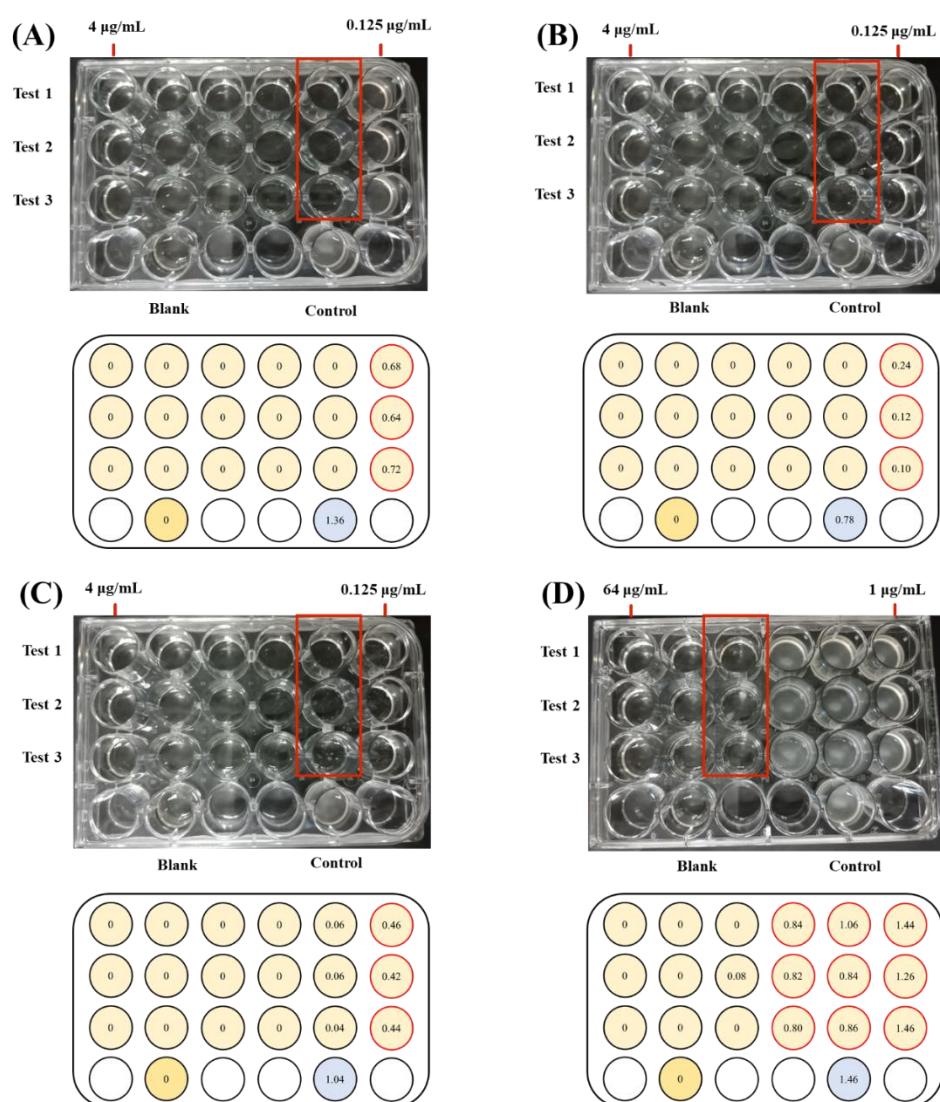


Figure S1. Corresponding photographs of the microdilution results by using oxacillin as the antibacterial agent against four model *S. aureus* strains, including (A) *S. aureus* clinical strain, (B) *S. aureus* BCRC 10823, (C) *S. aureus* BCRC 10831, and (D) MRSA. The red squares indicate where the determined MICs are. The highest and lowest concentrations were labeled on the top of the photographs to represent the 2-fold series dilution. The cartoon illustration showed the OD value obtained in each well. Tests 1-3 indicate three replicates.

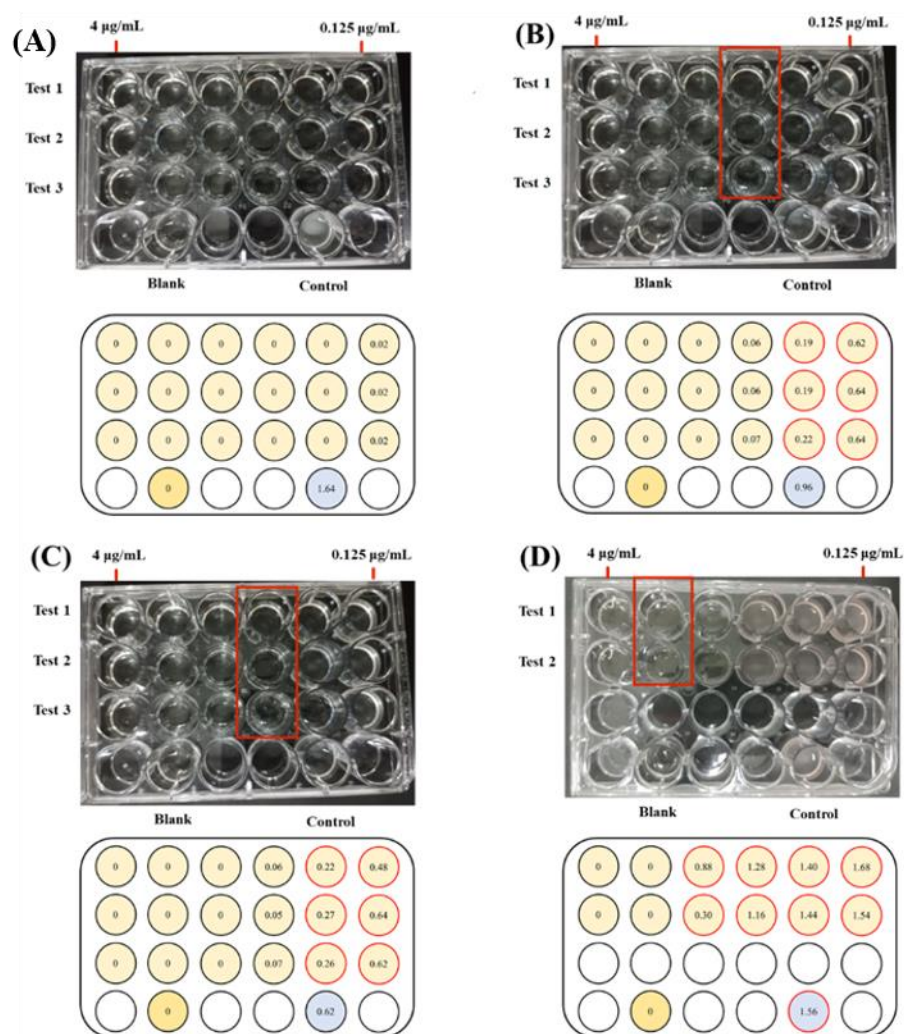


Figure S2. Corresponding photographs of the microdilution results by using vancomycin as the antibacterial agent against four model *S. aureus* strains, including (A) *S. aureus* clinical strain, (B) *S. aureus* BCRC 10823, (C) *S. aureus* BCRC 10831, (D) MRSA clinical strain. The red squares indicate where the determined MICs are. The highest and lowest concentrations were labeled on the top of the photographs to represent the 2-fold series dilution. The cartoon illustration showed the OD value obtained in each well. Tests 1-3 indicate three replicates.

References

1. Bright, J. J.; Claydon, M. A.; Soufian, M.; Gordon, D. B., Rapid typing of bacteria using matrix-assisted laser desorption ionisation time-of-flight mass spectrometry and pattern recognition software. *J. Microbiol. Methods* **2002**, *48*, 127-138.
2. Khot, P. D.; Fisher, M. A., Novel approach for differentiating *Shigella species* and *Escherichia coli* by matrix-assisted laser desorption ionization–time of flight mass spectrometry. *J. Clin. Microbiol.* **2013**, *51*, 3711-3716.
3. Tang, W.; Ranganathan, N.; Shahrezaei, V.; Larrouy-Maumus, G., MALDI-TOF mass spectrometry on intact bacteria combined with a refined analysis framework allows accurate classification of MSSA and MRSA. *PloS one* **2019**, *14*, e0218951.
4. Wang, H.-Y.; Chung, C.-R.; Wang, Z.; Li, S.; Chu, B.-Y.; Horng, J.-T.; Lu, J.-J.; Lee, T.-Y., A large-scale investigation and identification of methicillin-resistant *Staphylococcus aureus* based on peaks binning of matrix-assisted laser desorption ionization-time of flight MS spectra. *Briefings Bioinf.* **2021**, *22*, bbaa138.
5. Kong, P.-H.; Chiang, C.-H.; Lin, T.-C.; Kuo, S.-C.; Li, C.-F.; Hsiung, C.-A.; Shiue, Y.-L.; Chiou, H.-Y.; Wu, L.-C.; Tsou, H.-H., Discrimination of methicillin-resistant *Staphylococcus aureus* by MALDI-TOF mass spectrometry with machine learning techniques in patients with *Staphylococcus aureus* bacteremia. *Pathogens*. **2022**, *11*, 586.
6. Liu, X.; Su, T.; Hsu, Y. M. S.; Yu, H.; Yang, H. S.; Jiang, L.; Zhao, Z., Rapid identification and discrimination of methicillin-resistant *Staphylococcus aureus* strains via matrix-assisted laser desorption/ionization time-of-flight mass spectrometry. *Rapid Commun. Mass Spectrom.* **2021**, *35*, e8972.
7. Ciloglu, F. U.; Caliskan, A.; Saridag, A. M.; Kilic, I. H.; Tokmakci, M.; Kahraman, M.; Aydin, O., Drug-resistant *Staphylococcus aureus* bacteria detection by combining surface-enhanced Raman spectroscopy (SERS) and deep learning techniques. *Sci. Rep.* **2021**, *11*, 18444.
8. Yu, J.; Tien, N.; Liu, Y.-C.; Cho, D.-Y.; Chen, J.-W.; Tsai, Y.-T.; Huang, Y.-C.; Chao, H.-J.; Chen, C.-J., Rapid identification of methicillin-resistant *Staphylococcus aureus* using MALDI-TOF MS and machine learning from over 20,000 clinical isolates. *Microbiol. Spectrum* **2022**, *10*, e00483-22.